

INDUCTION VACUUM SMELTING OF Co-Al-W SUPERALLOYS – OPTIMIZING THE FEEDSTOCK BASED ON THE ALLOY'S CHEMICAL COMPOSITION, ELEMENTAL SEGREGATION, AND SLAG FORMATION

T. Mikuszewski ^a, A. Tomaszewska ^a, G. Moskal ^{a,b}, D. Migas ^{a*}, B. Witala ^{a,c}

^a Silesian University of Technology, Department of Materials Technologies, Katowice, Poland

^b Silesian University of Technology, University Zone of Material Innovations, Katowice, Poland

^c Silesian Aviation Technology Laboratory, Section for Advanced Materials and Protective Coatings Technologies for Aircraft Engines and Propulsion Systems, Katowice, Poland

(Received 07 November 2021; accepted 23 February 2022)

Abstract

In this study, the manufacturing of Co-Al-W alloys by smelting in a vacuum induction furnace was discussed taking into account the optimizing of the feedstock material morphology. Herein, the influence of various feedstock conditions and the order of introducing the alloying elements into a liquid alloy were analyzed and described. The investigation revealed that it was possible to obtain the desired chemical composition of Co-Al-W alloys using fragmented tungsten pellets introduced from a vacuum feeder into the liquid Co-Al alloy heated above the liquidus temperature to maximum of 40-50 °C. This technical variant required accurate temperature control of the molten alloy, which did not ensure complete reproducibility. The disadvantage of this process was a relatively high slag formation. The optimal technical solution involved obtaining the liquid Co-W solution and introducing Al at the end of the smelting process; in this variant, the slagging effect was relatively low. Additionally, melting of the alloy in an argon atmosphere reduced the loss of aluminum due to evaporation, as compared to melting in a vacuum. The smelting process could be carried out either in Al₂O₃ solid crucibles or in compacted crucibles made of MgO-based refractory mass.

Keywords: Co-Al-W alloys; Feedstock optimizing; Smelting process; Dendritic segregation; Chemical composition

1. Introduction

Alloys based on the Co-Al-W system can be presented as a new class of heat-resistant materials that have become the subject of intense scientific research. These materials are of particular interest in terms of microstructural modification because they have the potential to exhibit comparable or superior mechanical properties relative to Ni-based superalloys. Research conducted by Lee [1] in the 1970s revealed the possibilities embodied by a new group of precipitation-hardened Co-Al-X superalloys strengthened by L1₂ phase (i.e., Co₃(Al,X)). This discovery was developed by Sato et al. in 2006 [2]. The authors identified Co-based superalloys showing a high-temperature strength greater than those of conventional Co-based superalloys. A high level of high-temperature strength was caused by presence of the coherent L1₂ phases (with formula Co₃(Al,W)), precipitated in the disordered face-centered cubic cobalt matrix. Moreover, the discussed group of

alloys was characterized by a high melting point.

The results concerning the γ'-strengthened alloys led to the development of two main groups of Co-based superalloys containing aluminum. The Co-Al-W and W-free Co-Al-Mo-Nb/Ta alloys may be distinguished. Suzuki et al. [3] presented the first systematic investigation of Co-Al-W alloys. The study was related to Co-9Al-9W and Co-9Al-10W-2Ta alloys, and their temperature depended on flow stress. It was found that the strength of Co-Al-W-Ta quaternary alloys was comparable to that of the Ni-based superalloy at 1173 K. The polycrystalline and single-crystal Co-Al-W alloys with addition of Re, Cr, and Ta were also described by Suzuki and Pollock [4]. The high-temperature strength and deformation behavior of the γ/γ' double-phase alloys were studied. Mäkinen [5] published the first information about Co-10Al-5Mo-2Nb alloy. In the study, the metastable cuboidal Co₃(Al,Mo,Nb) phase was found as the main strengthening structural element. The precipitates were coherent with the face-centered cubic γ-Co

*Corresponding author: damian.migas@polsl.pl



matrix and was characterized by ordered $L1_2$ structure. The reported density the W-free alloys was lower than that of Co-Al-W.

In both cases, the Co-based alloys were strengthened by the γ' phase with $L1_2$ type lattice. The thermodynamic stability of this phase, as well as the chemical range of its formation, were determined by the presence of alloying elements. Xue et al. [6] found that Ti and Ta additions increased the γ' solvus temperatures of Co-Al-W-base alloys to 1131 and 1157 °C respectively. The similar result concerning Ti and Ta additions was confirmed by Omori et al. [7], as well as the beneficial effect of Nb on the γ' solvus. Shinagawa et al. [8] revealed that the solvus temperature of γ' could increase Ni alloying. Tomaszewska evaluated the microstructure of the Re-containing multicomponent Co-Ni-Al-W-Re-Ti alloy [9].

The development of alloy composition required producing multi-component alloys that contained alloying elements with different melting points. Such compositions were often a combination of high melting point elements and low melting point elements such as aluminum (e.g., Co-9Al-9W (at.%) alloy). Similar to Ni-based superalloys, the complex chemical composition often lead to a dendritic segregation of alloying elements in as-cast microstructures of castings. Moreover, eutectics could be formed, as well as various types of defects at grain boundaries. Shi et al. [10] published the research related to the solidification sequence, microstructural evolution, interdendritic segregation, and elemental distribution of as-cast IN718 alloy. The paper reveals the scale of the technological issues related to the casting of this type of alloys.

The solidification pathway and primary microstructure morphology of the as-cast alloys are critical aspects to consider when designing heat treatments. Moreover, an identification of these factors enables obtaining feedback concerning a technical processes of alloy manufacturing, including smelting and casting. They are particularly essential for a process correction and optimization. These issues have been thoroughly investigated for Ni-based superalloys, especially in terms of solidification pathways, micro- and macrosegregation of alloying elements, and the formation of undesirable eutectic regions. Zhang et al. [11] analyzed the microstructure evolution of Ni-based superalloys at a wide range of solidification cooling rate. Depending on solidification cooling rate, microstructures sequentially showed planar, cellular, dendritic, dendritic growth suppressed features, and the shapes of γ' precipitates progressively exhibited irregular, cuboidal, and spherical patterns. Homam et al. [12] used the Scheil equation to model the solidification path, microsegregation of alloying elements in the

interdendritic regions, solidification temperature ranges, prediction of the formation of secondary structures and the castability behavior of the as-cast superalloys.

However, there are limited publications characterizing the primary structure of Co-Al-W and W-free alloys or discussing the issue of eutectic formation. McDevitt [13] published the technological and microstructural characterization of the γ' -strengthened Co-Al-W-X superalloys melted using the vacuum induction process, as well as the alloys fabricated via the vacuum arc remelting. This paper presents experience in assessing the feasibility of manufacturing wrought billets. Koßmann et al. [14] characterized the microsegregation and solidification of a multi-component Co-based superalloy. The authors compared behavior of the multicomponent alloy to the ternary Co-Al-W alloy and to two exemplary Ni-based superalloys. They combined the experimental characterization of as-cast microstructures with complementary modelling of phase stability.

The aim of this study is the investigation of particular technical aspects concerning smelting of Co-9Al-9W alloys in a vacuum induction furnace. The effects of the feedstock materials morphology (I) and the method of introducing different components during smelting (II) were analyzed based on the chemical composition of the final alloy. The impact of using solid crucibles and compacted crucibles was evaluated, and the loss of refractory mass in the smelting process was discussed.

2. Experimental Procedures

The nominal chemical composition of the analyzed Co-based superalloy is shown in Table 1. The alloys were smelted in the Balzers VSG 02 laboratory vacuum induction furnace at various temperatures. The advantage of this furnace is the small capacity of a crucible (approx. 0.2 L), which allows the fabrication of small ingots at the initial stage of the tests, thus reducing the use of input materials. The smelting process was carried out in crucibles made of solid Al_2O_3 . Prior to the smelting, the furnace chamber was flushed three times with argon and subsequently pumped to the pressure of 10-3 Tr (~0.13 Pa). In the first phase of the metallurgical process, the smelting was under vacuum. After degassing of a liquid alloy, in the second phase of the metallurgical process, the smelting atmosphere contained argon (Ar; purity = 99.999%; ALPHAGAZTM), which filled the furnace chamber to the pressure of 600 Tr (~0.08 MPa). Pure metals were used as input components. Especially, the main feedstock materials were (I) cobalt (Fig. 1a) in the form of pressed powder pellets or the electrolytic



cobalt (min. 99.98% Co); (II) aluminum (grade AW – 99.98% Al); and (III) tungsten in the form of pressed and sintered pellets or high-purity solid rod shavings. The tungsten pellets were introduced with or without mechanical fragmentation (Fig. 1b).

Table 1. Nominal chemical composition of the Co-9Al-9W alloy

Element	Co	Al	W
at.%	82	9	9
wt.%	71.80	3.61	24.59



Figure 1. Morphology of (a) cobalt feedstock materials used for Co-9Al-9W alloy smelting: electrolytic cobalt (left) and pressed Co pellets (right), and (b) tungsten feedstock materials used for Co-9Al-9W alloy smelting: crushed W pellets (left) and uncrushed W pellets (right)

In this study, three methods of tungsten introduction were investigated in the stage I:

- Variant “1”: crushed tungsten pellets loaded into a crucible together with cobalt (pellets) and aluminum;
- Variant “2”: a raw tungsten loaded into a liquid Co-Al alloy using a vacuum feeder (Co pellets);
- Variant “3”: a shredded tungsten loaded into a liquid Co-Al alloy using a vacuum feeder (Co pellets).

The smelting temperature of the alloys was ~1650 °C or in the range from 1520 to 1530 °C (depending on the technical variant). The smelting time ranged

from 8 to 10 min. The alloys were casted into graphite molds under an argon atmosphere. The final product of the casting process were two rods with dimensions of $\varnothing 20 \times 100$ mm connected by a sprue (the shape of mold).

In stage II, the slag formation was analyzed for the following variants:

- Variant “3A” – tungsten pellets and a high-purity electrolytic cobalt were used for a Co-W alloy formation;
- Variant “3B” – high-purity tungsten rods and a high-purity electrolytic cobalt were used for a Co-W alloy formation;
- Variant “3C” – high-purity tungsten pellets and cobalt pellets were used for a Co-W alloy formation (in a two-stage process);
- Variant “3D” – high-purity tungsten pellets and cobalt pellets were used for a Co-W alloy formation (in a one-stage process).

In the first stage of this study, the effects of the smelting process were analyzed based on the morphology of the dosed components. In the second stage of the study, significant technological modifications to the metallurgical process were applied, including changing the order of introducing the batch components into a melt, and the impact of these changes was evaluated.

The scanning electron microscopy (SEM) technique was used to obtain images and conduct a chemical composition analysis of ingots using the Hitachi S-4200N scanning electron microscope equipped with an Energy Dispersive X-Ray Spectrometer (EDS). The microscopic observations of material cross-sections were performed using the Nikon Eclipse MA200 optical microscope.

3. Results

In the first stage of the investigation concerning the fabrication of Co-Al-W alloys, the three variants with different input components morphology were subjected to the smelting processes. The schematic showing the smelting process for each variant is shown in Fig. 2. Cobalt (in the form of pressed powder pellets), aluminum, and tungsten (in the form of pressed powder pellets, with and without a mechanical fragmentation) were used as input components.

The reason for the evaluation of such diversified feedstock forms was connected with the process of electrodynamic mixing of liquid metals during smelting. Particularly, the mixing of a molten metal generated a convex meniscus and drew a slag towards the walls of a crucible (Fig. 2a). This phenomenon allowed a formation of a region free of a slag on the smelted alloy's surface. Thus, the introduction of alloying additives (input components) into the mirror

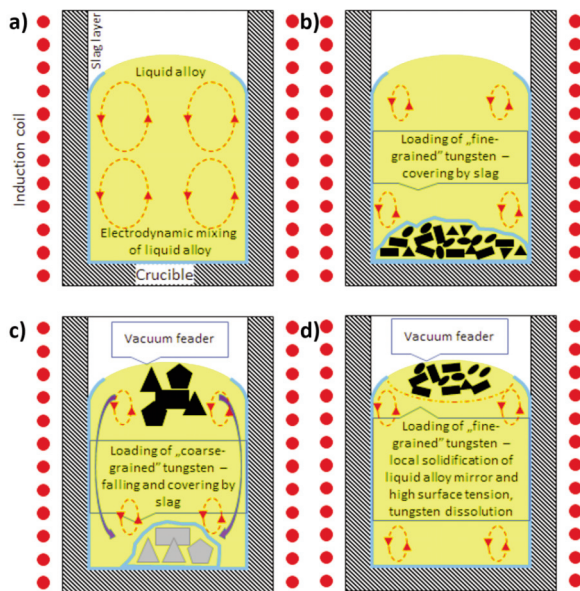


Figure 2. Technical diagrams of Co-9Al-9W alloy smelting. (a) conditions of the electromagnetic field generated by the inductor coil; (b) variant 1 - loading fragmented tungsten pellets into the crucible; (c) variant 2 - introducing non-fragmented tungsten pellets into the liquid Co-Al alloy from the vacuum feeder; (d) variant 3 - loading fragmented tungsten pellets into the liquid Co-Al alloy from the vacuum feeder

of a liquid metal prevented the undesirable effect wherein pieces of alloying input components got coated by a slag. The main component of the slag were aluminum oxides, which were formed on surface of Al pieces. A large surface area of the contact between the unobstructed metallic liquid alloy and the incorporated additives promoted their dissolution in the liquid alloy. This technical assumption was the basis for a selection of the analyzed variants and the method of feeding.

In the first variant, crushed tungsten pellets were used simultaneously with loading of the input components (Co, Al, W) into a crucible (Fig. 2b). The process of W dissolution could start after melting of Al and formation of the liquid Co-Al alloy. The tungsten pellets dropped to the bottom of the crucible may be covered with a slag layer. To avoid this issue, the smelting temperature was increased to approximately 1650 °C. After holding the liquid Co-Al-W alloy at this temperature for 7-8 min, the alloy was cast into the mold. Increasing the smelting time or temperature favored a transition of greater amounts of tungsten into the liquid alloy, whereas such changes were also associated with a successive loss of aluminum due to evaporation.

In the second variant, non-fragmented tungsten pellets were introduced into the the Co-Al solution from a vacuum feeder (after creating a slag-free mesh

on the alloy mirror (Fig. 2c)). Unfortunately, due the specific weight of tungsten substantially higher than that of the Co-Al alloy, large pieces of W feedstock component fell to the bottom of the crucible and remained undissolved. The smelting process was carried out at 1650 °C for approximately 10 minutes. Analysis of the material which remained at the bottom of the crucible after casting indicated that the nominal chemical composition of the alloy was not achieved. The later studies revealed that there was approximately 24 wt.% loss of Al compared to that of the weight of the initial batch.

After several preliminary tests, in which the size of tungsten pieces and the temperature of the liquid Co-Al alloy were altered, the third variant was examined. This experiment involved introducing fragmented tungsten pellets into the liquid Co-Al alloy from a vacuum feeder (Fig. 2d). It was determined that the optimal results were obtained using the tungsten pellets after fragmentation. The fragments ranged in size from 5-7 mm, and the temperature range of the liquid alloy was maintained between 1520-1530 °C.

The introduction of fragmented tungsten pellets into the mirror of a liquid metal that was mostly free of the slag and caused a localized solidification of the liquid alloy. The tungsten pellets (surrounded by a locally-solidified alloy) remained on the surface because of a high surface tension. This factor prevented tungsten pellets from falling to the bottom of the crucible and an interaction with a slag. Maintaining a slight overheating temperature reduced the evaporation of aluminum and allowed direct observation of the gradual dissolution of tungsten pellets in the liquid alloy. Approximately 10 minutes after the tungsten pellets were introduced into the liquid batch, they were dissolved, and the melt was cast into a mold.

The main challenge associated with the described technical methods was the inability to remove slag from the surface of the liquid alloy before introducing tungsten from a vacuum feeder. A small portion of the introduced tungsten inevitably fell into the slag present on the liquid alloy mirror and gets coated. The slagged pieces of the tungsten component fell to the bottom of the crucible and remained partially undissolved. This was a random phenomenon, therefore, there was no possibility to verify how much of tungsten could get in contact with the slag. Furthermore, it was difficult to control the amount of tungsten being incorporated into the alloy without falling to the bottom of the crucible.

It should also be noted that the described technical procedures were implemented using the specific furnace parameters and the coil supply current conditions. The experiments were conducted using a total batch weight of approximately 800 g. The

crucible capacity was approximately 200 mL; the size of tungsten pieces were in accordance with the conditions mentioned above. When modifying the conditions of the metallurgical process (e.g., crucible size, batch mass, frequency of the coil supply current), it was necessary to select other experimental parameters to obtain optimal smelting results.

After the smelting process, the chemical compositions of the obtained alloys (generated by the procedures described for each variant) were determined (Fig. 2b-d). The measurements were carried out on samples acquired from the middle of the casted rods. The observations were made on a plane perpendicular to an axis of a rod, at three designated measuring points (i.e., on the edge, in the middle of the radius, and in the center of the cross-section). The results of the analysis are available in Table 2.

Table 2. Chemical composition of Co-9Al-9W alloys obtained using the described technical conditions for variants 1, 2, and 3

Technical variant	Place of analysis in the sample	Element [at.%]		
		Co	Al	W
Crushed tungsten introduced into the crucible (variant 1; Fig. 4b)	Edge	85.8 ± 1.2	6.9 ± 0.3	7.3 ± 0.4
	Half radius	85.8 ± 1.1	6.9 ± 0.2	7.3 ± 0.4
	Center	85.9 ± 1.2	6.9 ± 0.3	7.2 ± 0.4
Non-crushed tungsten introduced from a vacuum container (variant 2; Fig. 4c)	Edge	87.4 ± 1.3	6.2 ± 0.2	6.4 ± 0.3
	Half radius	87.2 ± 1.3	6.5 ± 0.3	6.3 ± 0.2
	Center	87.9 ± 1.4	6.2 ± 0.2	5.9 ± 0.3
Crushed tungsten introduced from a vacuum container (variant 3; Fig. 4d)	Edge	81.7 ± 1.0	8.8 ± 0.3	9.5 ± 0.5
	Half radius	82.2 ± 1.2	8.7 ± 0.3	9.1 ± 0.4
	Center	82.5 ± 1.2	8.5 ± 0.3	9.0 ± 0.4

The data presented in Table 2 indicates that the variant involving introduction of fragmented tungsten pellets from a vacuum feeder into the liquid Co-Al alloy (variant 3), led to production of Co-9Al-9W alloy with the chemical composition close to the nominal one (82:9:9 atomic ratio of Co:Al:W).

The distribution of alloying elements implied that the addition of crushed tungsten dose directly to the liquid Co-Al bath resulted in the desired primary structure of the Co-9Al-9W alloy with a high degree of homogeneity. This effect was confirmed by the

homogeneous distribution of tungsten and aluminum in dendritic and interdendritic regions (Fig. 3a, Fig. 3b, Table 3).

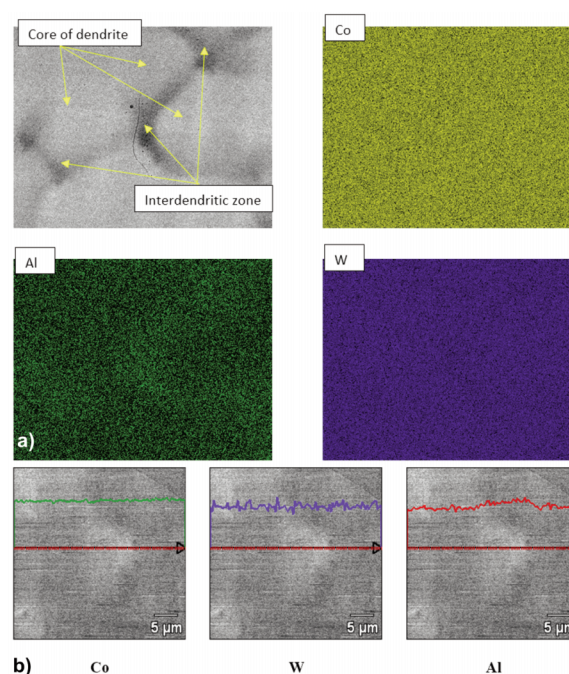


Figure 3. (a) Chemical composition of dendritic and interdendritic zones in a Co-Al-W alloy (variant 3) in regions of equiaxed crystals – maps of alloying elements distribution. (b) Chemical composition of dendritic and interdendritic zones in Co-Al-W alloy (variant 3) in regions of equiaxed crystals – linear distribution of alloying elements

Table 3. Chemical composition in dendritic and interdendritic zones of Co-9Al-9W alloys obtained in the described technical conditions of variant 2

at.%	Co	Al	W	Co	Al	W
	Dendritic zone			Interdendritic zone		
Average concentration	84.5	7.1	8.4	82.6	8.7	8.7
Maximum	84.8	7.6	8.7	83.7	9.6	9.0
Minimum	83.7	6.7	8.2	81.9	7.7	8.5
Standard deviation	0.5	0.4	0.2	0.7	0.7	0.2

This observation could be applied primarily to tungsten, whose distribution in the primary microstructure was a critical technical problem and required an additional homogenizing treatment. The data obtained in these studies suggested that the difference in W concentration between dendritic and interdendritic spaces did not exceed a maximum value of 0.7 at.%. The discussed microsegregation included the areas of equiaxed crystals; however, the

differences in tungsten concentration were much smaller in the columnar crystal zones. More significant differences were observed in the content of aluminum and cobalt. The overall view of the as-cast microstructures in the areas of columnar and equiaxed grains (in the case of the optimal variant) is shown in Fig. 4. The data presented in Table 3 reveals that the most beneficial effect related to chemical homogeneity was obtained owing to the tungsten distribution, where the standard deviation was the lowest for both dendritic and interdendritic zones.

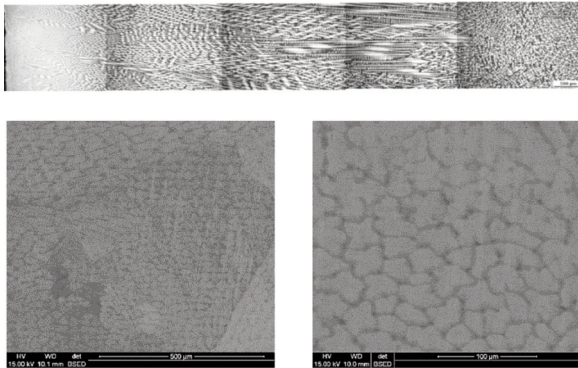


Figure 4. Overall view of the primary microstructure of the optimal Co-9Al-9W alloy in the as-cast condition (top) with details from columnar (bottom left) and equiaxed zones (bottom right)

After carrying out several preliminary smelting tests, it was discovered that solid crucibles made of sintered Al_2O_3 exhibit two disadvantages. First, the thin walls of these crucibles often break off during the annealing and degassing processes that occurred before smelting. These cracks did not disqualify the crucibles, since they were mounted in the coil using a refractory mass, and there was no risk that the liquid alloy could penetrate the coil. However, the cracked pieces of the crucible made the casting process casting more complicated and could contaminate an alloy. Secondly, it was difficult to remove alloy residues from a crucible after the casting process due to penetration of the cracks by a molten metal. For these reasons, crucibles made from tamped and sintered refractory mass (MgO matrix) were employed to verify other potential options for smelting the Co-9Al-9W alloy. It was determined that despite the developed inner surface of the crucible, it was relatively simple to remove metal residues from these compacted crucibles after casting. After the adequately conducted metallurgical process (optimal technical variant 3; Fig. 2d), a thin residue remained in the crucible made of the compacted refractory mass (Fig. 5a). For comparison, the alloy was cast using the method described for technical variant 2 (Fig. 2b), and it was recognized that a compact mass of slag and tungsten remained at the bottom of the Al_2O_3 crucible.

Ultimately, this residue could not be mechanically removed from the crucible (Fig. 5b).

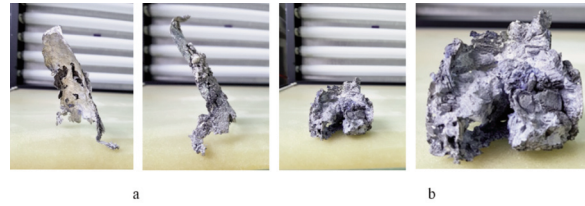


Figure 5. Residues of Co-9Al-9W alloy after casting. (a) smelting in a crucible of tamped and sintered refractory mass (optimal metallurgical process for variant 3; Fig. 2d); (b) smelting in an Al_2O_3 crucible according to the scheme in Fig. 2b

The durability of crucibles made from refractory mass was comparable to that of crucibles made from Al_2O_3 , which were usable for several melts. It is worth to notice that crucibles made of refractory mass are cheaper than crucibles made of Al_2O_3 , and the tamped and sintered mass can be partially recovered after breaking the lining and then used for tamping of subsequent crucibles. The disadvantage of using compacted crucibles is the labor-intensive and time-consuming nature of their preparation. For example, a compacted crucible requires several hours of heating to sinter the mass, long-term degassing in a vacuum, and implementation of rinsing heats before an actual melting process. Therefore, it can be concluded that the MgO-based tamped refractory crucibles are a viable alternative to solid Al_2O_3 crucibles; however, their use does not provide substantial benefits.

The analysis concerning the first stage of this study showed that it was feasible to obtain Co-9Al-9W alloy with the nominal chemical composition by using the strictly controlled smelting parameters (temperature and time) and by introducing crushed tungsten pieces into the liquid Co-Al solution. However, the multiple smelting processes showed that the smelting was not completely reproducible. Due to small differences in technical parameters, various amounts of a residual slag remained in the crucible together with a post-slag residue. As a consequence, the obtained alloys exhibited deviations from the nominal chemical composition.

A slag plays a particularly important negative role in the process of Co-9Al-9W alloys smelting. Therefore, the objective of the second stage of the research was to determine the source of a slag formed during the smelting process, which hindered the dissolution of tungsten in the liquid alloy. It can be assumed that pressed powder pellets of cobalt were the main source of the slag. Therefore, this component was replaced in the first two melts with more expensive cobalt in the form of electrolytically refined plates (Fig. 1a).

The first smelting process (3A) was carried out in

accordance with the optimal technical scheme, established in the first stage of this research (variant 3; Fig. 2d), using high purity electrolytic cobalt. During smelting, some slag was observed immediately after obtaining the liquid Co-Al solution. It was not likely to obtain a completely clean, slag-free mirror of the liquid alloy, even under the strong magnetic field of the coil. After introducing the crushed tungsten from a vacuum feeder, several pieces were surrounded by slag residues from the surface. As a result, the pieces were only partially dissolved in the liquid melt. Therefore, the tungsten content was lower than the expected one, and a relatively high aluminum concentration was present in the ingot (Table 4).

The second smelting process (3B) was carried out in two stages. In the first step, electrolytic cobalt plates were placed in a crucible and smelted. No slag was observed on the surface of the liquid metal. Subsequently, a high purity tungsten feedstock was introduced from a vacuum feeder, and after waiting for approximately 5 minutes, there was still no slag on the surface of the liquid alloy. The alloy was then poured into the mold. On the upper surface of the ingot, the macrostructure displayed a color contrast; minimal amounts of slag aggregates were clearly visible (Fig. 6a). In the second step, the ingot was mechanically cleaned and placed back into the crucible. After the ingot was melted, no slag was observed on the surface of the liquid alloy. Aluminum was introduced into the liquid alloy from a feeder; then, a layer of slag appeared on the surface of the liquid alloy immediately after its dissolution. After waiting for approximately two minutes, the alloy was poured into the mold (Fig. 6b). At this point, it was discovered that the surface of the ingot was completely covered with a dense layer of slag. The analysis of the chemical composition revealed that the

deviation from the nominal composition was much smaller than that of the previous melt, 3A (Table 4).



Figure 6. (a) Co-W alloy ingot obtained during 3C process; (b) final Co-9Al-9W alloy ingot obtained during 3C process

The third smelting process (3C) was carried out in a similar way as the 3B process. The difference between the processes was that cheaper input feed components were used in the 3C process, i.e. cobalt and tungsten, both in the form of pressed powder pellets. However, the results concerning the smelting process were similar to those obtained during the 3B smelting.

The primary disadvantage of the 3B and 3C smelting variants was the two-stage metallurgical process (i.e. first stage – smelting the Co-W alloy ingot; Second stage – introducing aluminum and final casting of the Co-9Al-9W alloy ingot). Therefore, the fourth smelting process (3D) was carried out in a single step. The Co and W pellets were placed in a crucible, and aluminum was introduced into the liquid Co-W alloy from a vacuum feeder. Similarly to the previous melts, the slag appeared only after the introduction of Al into the molten alloy. The chemical composition of the obtained ingot is provided in Table 4.

Table 4. Chemical composition of Co-9Al-9W alloys obtained in the second stage of investigations

Variant	Area of analysis	Element [at.%]			Mass [g]		
		Co	Al	W	Ingot	Residue	Mass gain
3A	Edge	82.6 ± 1.2	9.7 ± 0.5	7.7 ± 0.2	485	93	22
	Half radius	82.3 ± 1.1	10.0 ± 0.6	7.8 ± 0.3			
	Center	81.8 ± 1.0	10.6 ± 0.6	7.5 ± 0.2			
3B	Edge	82.0 ± 1.3	9.8 ± 0.4	8.5 ± 0.2	528	53	19
	Half radius	81.8 ± 1.2	9.4 ± 0.4	8.8 ± 0.4			
	Center	82.1 ± 1.2	9.5 ± 0.3	8.4 ± 0.2			
3C	Edge	82.8 ± 1.4	8.9 ± 0.3	8.3 ± 0.2	562	29	9
	Half radius	82.7 ± 1.0	8.9 ± 0.2	8.4 ± 0.4			
	Center	82.9 ± 0.9	8.9 ± 0.3	8.2 ± 0.2			
3D	Edge	82.0 ± 1.3	8.6 ± 0.2	9.4 ± 0.5	552	48	0
	Half radius	82.5 ± 1.2	8.7 ± 0.3	8.9 ± 0.2			
	Center	82.7 ± 1.2	8.4 ± 0.2	9.0 ± 0.4			



It should be noted that during the 3B, 3C, and 3D smelting processes, the temperature and time of the process were not rigorously controlled, as they were in the 3A variant process (using the optimal variant from the first stage of the research). The melting and casting temperatures for the latter three procedures were 1550 ± 20 °C, and the total melting times ranged from 8 – 12 minutes. Despite these parameters, improved results were obtained following these processes in terms of reaching the target allow chemical composition.

4. Summary

Smelting and casting of Co-Al-W alloys can be carried out using various metallurgical equipment. However, considering the need to ensure adequate purity of the alloys, it was beneficial to use furnaces with a protective atmosphere (e.g., vacuum or argon), which reduced a risk of a contamination of the alloys with gases and non-metallic particles. Following a properly conducted metallurgical process, it was also possible to avoid the use of master alloys and use pure metals. Among the furnaces which enabled melting under a protective atmosphere, vacuum induction furnaces were particularly advantageous. In these furnaces, intense electrodynamic mixing of the liquid alloy occurred under the influence of the electromagnetic field generated by the inductor (coil). This process ensured both thermal and chemical homogenization of the alloy. If the alloying elements were not very reactive (e.g., Ti, V), ceramic crucibles could be implemented in the smelting processes, regardless of whether they were solid or tamped and sintered from refractory masses. The discussed alloys could be cast into permanent metal or graphite molds, as well as into semi-permanent or disposable ceramic molds.

The general technical schematic describing the smelting process of Co-9Al-9W alloys and other cobalt-based alloys in vacuum induction furnaces is depicted in Fig. 7.

Taking into account smelting and casting of metal alloys (including cobalt alloys), the appropriate selection and preparation of feedstock materials is essential (Fig. 8). The type and preparation of the charge often have the significant influence on the quality of castings and ingots. Due to the closed, hermetic smelting chamber in vacuum furnaces, it was difficult to implement the refining processes, which were completed with a slag removal. The alloys features such as chemical composition and particularly the content of inclusions and impurities depended primarily on the purity of feedstock components used in the smelting process. Taking into consideration the specificity of the discussed metallurgical furnaces, numerous technical

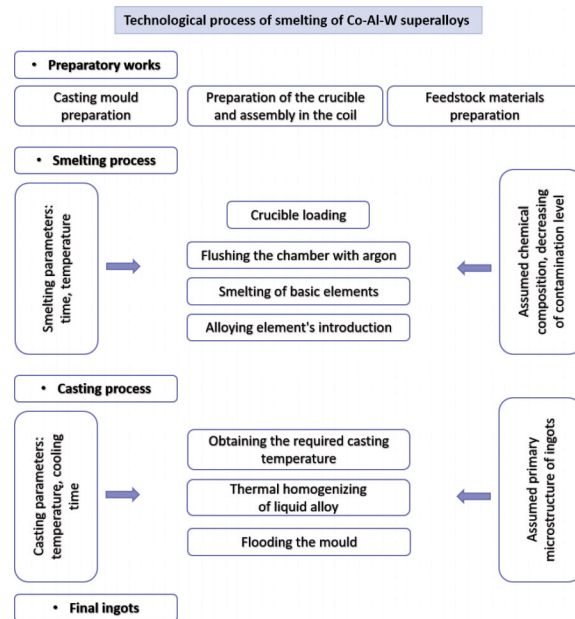


Figure 7. General technical schematic of smelting the Co-9Al-9W alloy and other cobalt-based alloys in a vacuum induction furnace

recommendations related to implementing new smelting processes for obtaining Co-based alloys in a vacuum or a protective atmosphere could be made (see Fig. 8):

- Apply qualified charge metals with the highest possible purity in the smelting process. If recycled scrap metal is used, it is necessary to consider skimming alloy components during re-smelting. Determining the specific amounts of admixtures and impurities that can be introduced into the alloy along with specific input components (e.g., with mortars and modifiers (if used)) is also required;

- Carefully prepare the charge materials prior to the smelting process – the charge preparation should include cleaning and drying, which are particularly important if using recycled scrap, oil-contaminated chips, etc. The alloying additions should be comminuted and fractionated. Introduction of charge pieces with significantly different dimensions may result in deviations from a nominal chemical composition of the alloys. For example, the extended dissolution time of large portions of the charge in the liquid melt may cause smaller pieces to dissolve and evaporate.

- Determine the method of charge materials loading and the dosing sequence of the alloying elements during smelting. If a construction of the vacuum furnace allows for dosing the alloy components during smelting, the optimal partitioning should be determined in terms of the charge materials and the components placed in a crucible before smelting. The components must be added in correct

amounts and dosed in a correct sequence during smelting. In general, the feedstock materials should be introduced into the liquid alloy in an increasing reactivity order (e.g., adding titanium and vanadium last, due to their reactivity with the ceramic crucibles and linings) and increasing vapor pressure (e.g., manganese should be introduced at the end of the smelting process to avoid an intense evaporation). Additionally, modifiers with a limited period of effective action should be added at the end of the smelting process. Components prone of rapid oxidation should be introduced into the liquid alloy after the de-oxidation. For example, pieces of chromium covered with a layer of oxides essentially do not dissolve in some liquid alloys, such as molten copper; therefore, it is necessary to introduce deoxidizers, such as silicon, into the melt first. Following the correct order of introducing components into the melt, while maintaining a predetermined temperature of the liquid solution, may also influence the sequence of the melt crystallization (the type of primary phases and the order of their formation). The examples of this effect include oxides, phosphides (e.g., AlP in silumin) or carbides (e.g., in copper and its alloys), which are formed after combining with metals introduced previously into the alloy. These phases are often heterogeneous nucleation pads that facilitate the nucleation of other primary phases and contribute to the fragmentation of the primary structure. The introduction of various alloying elements in the solidus-liquidus temperature range, after prior crystallization of the desired primary phases, can provide beneficial effects.

- Apply refining methods accounting for the specificity of construction and principles of operation of vacuum furnaces – due to the impracticability of conventional refining methods and the possibility of slag removal before casting, alloys smelted in vacuum furnaces may be refined to a limited extent. Specifically, gases and volatile impurities can be removed by high vacuum re-melting. When using induction furnaces, it is advisable to turn off the power before casting to allow the slag to rise to the surface. Slow casting helps to keep the slag layers in the crucible and may ease their later removal from the crucible after casting the alloy into the molds. It is preferable to use refining re-melts along with skinning the ingots after each casting to remove the surface slag coatings.

- Use a vacuum and protective atmospheres rationally – a vacuum should be applied in the initial smelting phase to remove gases and moisture from the melt space, and to remove volatile impurities from the liquid melt. In the second smelting phase, it is advantageous to continue the smelting process under a protective gas atmosphere (most often argon), which slows the evaporation of the alloying elements. The

increased pressure in the working chamber of the furnace also reduces the unfavorable phenomenon of internal evaporation (“cooking”) and ejection of the liquid alloy from the crucible. Further, it reduces the gassing effect of castings and ingots after pouring the alloy into the molds. The presence of a protective gas in the working chamber improves a thermal stability of the liquid alloy by absorbing the heat of exothermic reactions occurring during the fusion of certain alloying elements (e.g., aluminum and nickel). The heat resistance of refractory materials is higher in a protective gas atmosphere than in a vacuum, which enables significant overheating of the alloy without the risk of degrading these materials during smelting.

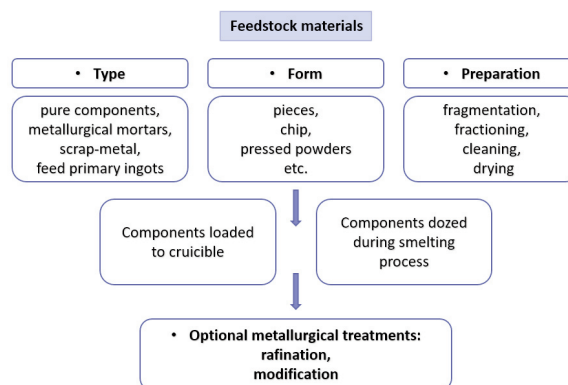


Figure 8. General scheme of feedstock material preparation and dosing during smelting processes

5. Conclusions

- Smelting of the Co-9Al-9W alloy in a vacuum induction furnace can be accomplished by using technically pure metals as input components. In this case, no master alloys are necessary.

- The chemical composition of the alloy, similar to the nominal composition, can be obtained by using fine-grained pieces of tungsten, introduced from a vacuum feeder into the liquid Co-Al solution, slightly overheated above the liquidus temperature (1520 – 1530 °C).

- It is necessary to strictly observe the melting parameters in the developed technical variant in order to limit a detrimental effect of a slag. The final result depends on the probability of slag removal from the surface of the liquid alloy before introducing tungsten.

- Aluminum is the source of a slag that hinders the dissolution of tungsten in the liquid cobalt alloy, even though this component has a high purity (99.98%) of. Therefore, the procedure was modified to dissolve tungsten in the molten alloy before formation of a slag resulting from Al dissolution.

- The optimal technical variant of smelting the Co-

9Al-9W alloy is based on the introduction of aluminum into the previously obtained liquid Co-W alloy.

• During the smelting of the Co-9Al-9W alloy, it is possible to use crucibles made of tamped and sintered loose refractory mass based on MgO, as a substitute for crucibles made of Al₂O₃.

Acknowledgements

This work is financed from the budgetary funds for science for the years 2018-2022, as a research project within the Diamond Grant programme (0069/DIA/2018/47).

Conflict of interest statement

On behalf of all authors, the corresponding author states that there is no conflict of interest.

Author's contribution

Tomasz Mikuszewski: Supervision, Investigation, Conceptualization, Methodology, Writing – original draft; Agnieszka Tomaszewska: Visualisation; validation; Grzegorz Moskal: Conceptualization, Formal analysis; Damian Migas: Project administration, Funding Acquisition, Writing – review & editing; Bartosz Witala: investigation.

Data availability

The data that support the findings of this study are available from the corresponding author upon reasonable request.

References

- [1] C.S. Lee, Precipitation-hardening characteristics of ternary cobalt – aluminium – X alloys, PhD Thesis, University of Arizona (1971).
<https://repository.arizona.edu/handle/10150/287709>.
- [2] J. Sato, T. Omori, I. Ohnuma, R. Kainuma, K. Ishida, Cobalt-base high-temperature alloys, *Science*, 312 (2006) 90-91.
<https://doi.org/10.1126/science.1121738>
- [3] A. Suzuki, G.C. Denolf, T.M. Pollock, Flow stress anomalies in γ/γ' two-phase Co–Al–W-base alloys, *Scripta Materialia*, 56 (2007) 385-388.
<https://doi.org/10.1016/j.scriptamat.2006.10.039>
- [4] A. Suzuki, T.M. Pollock, High-temperature strength and deformation of γ/γ' two-phase Co–Al–W-base alloys, *Acta Materialia*, 56 (2008) 1288-1297.
<https://doi.org/10.1016/j.actamat.2007.11.014>
- [5] S.K. Makineni, B. Nithin B, K. Chattopadhyay, Synthesis of a new tungsten-free $\gamma-\gamma'$ cobalt-based superalloy by tuning alloying additions, *Acta Materialia*, 85 (2015) 85-94.
<https://doi.org/10.1016/j.actamat.2014.11.016>
- [6] F. Xue, H.J. Zhou, X.F. Ding, M.L. Wang, Q. Feng, Improved high temperature γ' stability of Co–Al–W-base alloys containing Ti and Ta, *Materials Letters*, 112 (2013) 215-218.
<https://doi.org/10.1016/j.matlet.2013.09.023>
- [7] T. Omori, K. Oikawa, J. Sato, I. Ohnuma, U.R. Kattner, R. Kainuma, K. Ishida, Partition behavior of alloying elements and phase transformation temperatures in Co–Al–W-base quaternary systems, *Intermetallics*, 32 (2013) 274-283.
<https://doi.org/10.1016/j.intermet.2012.07.033>
- [8] K. Shinagawa, T. Omori, J. Sato, K. Oikawa, I. Ohnuma, R. Kainuma, K. Ishida, Phase Equilibria and Microstructure on γ' Phase in Co–Ni–Al–W System, *Materials Transactions*, 49 (6) (2008) 1474-1479.
<https://doi.org/10.2320/matertrans.MER2008073>
- [9] A. Tomaszewska, Primary microstructure characterization of Co-20Ni-9Al-7W-3Re-2Ti superalloy, *Journal of Mining and Metallurgy Section B Metallurgy*, 58 (1) (2022) 43-49.
<https://doi.org/10.2298/JMMB210309044>
- [10] Z. Shi, J. Dong, M. Zhang, L. Zheng, Solidification characteristics and segregation behavior of Ni-based superalloy K418 for auto turbocharger turbine , *Journal of Alloys and Compounds*, 517 (2013) 168-177. <https://doi.org/10.1016/j.jallcom.2013.03.241>
- [11] Y. Zhang, Y. Huang, L. Yang, J. Li, Evolution of microstructures at a wide range of solidification cooling rate in a Ni-based superalloy, *Journal of Alloys and Compounds*, 570 (2013) 70-75.
<https://doi.org/10.1016/j.jallcom.2013.03.085>
- [12] N.M. Homam, A. Mohammad-Reza, S. Seyed Hossein, M.A. Carlo, A solidification model for prediction of castability in the precipitation-strengthened nickel-based superalloys, *Journal of Materials Processing Technology*, 213 (2013) 1875-1884.
<https://doi.org/10.1016/j.jmatprotec.2013.04.019>
- [13] E. McDevitt, Vacuum induction melting and vacuum arc remelting of Co–Al–W–X gamma-prime superalloys, *MATEC Web of Conferences*, 14(2014) 02001.
<https://doi.org/10.1051/mateconf/20141402001>
- [14] J. Koßmann, C. H. Zenk, I. Lopez-Galilea, S. Neumeier, A. Kostka, S. Huth, W. Theisen, M. Göken, R. Drautz, T. Hammerschmidt, Microsegregation and precipitates of an as-cast Co-based superalloy—microstructural characterization and phase stability modelling, *Journal of Materials Science*, 50 (2015) 6329-6338.
<https://doi.org/10.1007/s10853-015-9177-8>



INDUKCIONO VAKUUMSKO TOPLJENJE Co-Al-W SUPERLEGURA – OPTIMIZACIJA SIROVINE NA OSNOVU HEMIJSKOG SAŠTAVA LEGURE, SEGREGACIJE ELEMENATA I FORMIRANJA ŠLJAKE

T. Mikuszewski ^a, A. Tomaszewska ^a, G. Moskal ^{a,b}, D. Migas ^{a*}, B. Witala ^{a,c}

^a Šleski tehnološki univerzitet, Odsek za tehnologije materijala, Katowice, Poljska

^b Šleski tehnološki univerzitet, Univerzitetska zona materijalnih inovacija, Katowice, Poljska

^c Šleska laboratorija za vazduhoplovnu tehnologiju, Sekcija za napredne tehnologije materijala i zaštitnih premaza za avionske motore i pogonske sisteme, Katowice, Poljska

Apstrakt

U ovom radu je razmatrana proizvodnja Co-Al-W legura topljenjem u vakuumskoj indukcionoj peći uzimajući u obzir optimizaciju morfologije sirovine. Analiziran je i opisan uticaj različitih uslova, kao i redosled uvođenja legirajućih elemenata u tečnu leguru. Ispitivanja su pokazala da je moguće dobiti željeni hemijski sastav Co-Al-W legura korišćenjem fragmentovanog peleta volframa koji se dodaje iz vakuumnog dodavača u tečnu Co-Al leguru zagrejanu iznad temperature likvidusa do maksimalno 40-50 °C. Ova tehnička varijanta zahteva preciznu kontrolu temperature rastopljenje legure, što nije osiguralo potpunu reproduktivnost. Nedostatak ovog postupka se ogleda u relativno velikoj količini formirane šljake. Optimalno tehničko rešenje podrazumeva dobijanje tečnog Co-W rastopa i uvođenje Al na kraju procesa topljenja; tokom ovog postupka količina formirane šljake je relativno mala. Pored toga, topljenje legure u prisustvu argona smanjuje gubitak aluminijuma usled isparavanja u poređenju sa topljenjem u vakuumu. Postupak topljenja se može izvršiti u loncima na bazi Al₂O₃ ili MgO.

Ključne reči: Co-Al-W legure; Optimizacija sirovine; Postupak topljenja; Dendritna segregacija; Hemijski sastav

